A Monolithic *Ka*-Band HEMT Low-Noise Amplifier

CINDY YUEN, CLIFFORD K. NISHIMOTO, MICHAEL W. GLENN, MEMBER, IEEE, YI-CHING PAO, ROSS A. LARUE, ROBERT NORTON, MEMBER, IEEE, MARY DAY, IRENE ZUBECK, STEVE G. BANDY, AND GEORGE A. ZDASIUK, MEMBER, IEEE

***Abstract*—A monolithic, single-stage HEMT low-noise amplifier has been developed for the 20–40 GHz band. This amplifier includes a single 0.25-μm-gate-length HEMT active device with on-chip matching and biasing circuits. A gain of approximately 6 dB from 20 to 38 GHz and a noise figure of approximately 5 dB from 26.5 to 40 GHz were measured. Replacing the triangular gate profile by a mushroom gate profile in the amplifier increased the measured gain to 8 dB from 20 to 37 GHz and reduced the measured noise figure to 4 dB from 26 to 40 GHz. These are the best reported results for a MMIC amplifier over this bandwidth. The chip size is 2.2 mm × 1.1 mm. The same amplifier was fabricated on pseudomorphic HEMT material with a triangular gate profile and has achieved 7.5 dB gain across the 20–35 GHz bandwidth and a 6.0 dB noise figure from 26.5 to 40 GHz. The measured 1 dB compression powers at 30 GHz for the conventional and pseudomorphic HEMT amplifiers are 10 dBm and 11.5 dBm, respectively, when biased for maximum power.**

I. Introduction

HEMT'S HAVE demonstrated superior gain and noise figure performance over conventional MESFET's [1]–[3]. State-of-the-art gain and noise performance has been achieved from monolithic amplifiers [4] and from hybrid amplifiers [5] using HEMT's at frequencies below 20 GHz. In *Ka*-band, reports have been made on monolithic amplifiers using MESFET's as active devices [6]–[9] and hybrid amplifiers have been developed using HEMT devices for low-noise applications [10]–[12].

This paper describes the first monolithic, reactively matched *Ka*-band low-noise amplifier using a 0.25 μm HEMT as the active device. The amplifier has achieved approximately 6 dB gain from 20 to 38 GHz and a 5 dB noise figure from 26.5 to 40 GHz. By replacing the triangular gate profile with a mushroom gate profile, the amplifier achieved 8 dB gain from 20 to 37 GHz with a 4 dB noise figure from 26 to 40 GHz, the best MMIC results reported to date. The same amplifier with a triangular gate profile was fabricated on the pseudomorphic HEMT material and has achieved higher gain (7.5 dB) at the expense of a narrower bandwidth (20–35 GHz) with a 6 dB noise figure from 26.5 to 40 GHz.

II. Device Considerations

Fig. 1 shows the HEMT expitaxial growth structure used in this amplifier. These HEMT layers were grown by MBE at 580°C on GaAs which was unintentionally doped n-type at about $1 \times 10^{14}/\text{cm}^3$. A five-period AlAs/GaAs superlattice is grown midway into the buffer layer in an attempt to reduce dislocations, improve surface morphology, and thereby improve the device noise performance.

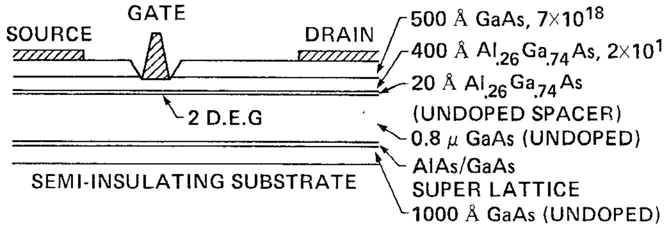

Fig. 1. Cross section of HEMT device.

The *I–V* characteristics of a discrete 0.25 μm × 150 μm HEMT are shown in Fig. 2. The gate is Π-configured with a triangular gate profile and the source–drain spacing is 2.5 μm. This device has a typical I_{dss} of 170 mA/mm, a g_m of 520 mS/mm at maximum gain bias and 380 mS/mm at minimum noise bias, a pinch-off voltage of 0.8 V, and a breakdown voltage of 5 V. The sheet density of the two-dimensional electron gas is approximately $2 \times 10^{12}/\text{cm}^2$. Fig. 3 shows the equivalent circuit model for this HEMT biased for minimum noise figure. The device was first characterized by the *S*-parameter measurements in the common-gate, common-source, and common-drain configurations from 2 to 18 GHz. An equivalent circuit model is then constrained to fit the three sets of data.

This 0.25 μm × 150 μm HEMT has a measured minimum noise figure of 1.35 dB and an associated gain of 12 dB at 18 GHz. The modeled F_{min} is 2.74 dB at 40 GHz. A *MAG* of 8 dB was measured at 38 GHz, which extrapolates to a f_{max} of about 101 GHz.

III. Circuit Design

A 20–40 GHz reactively matched amplifier was designed using a single 0.25 μm × 140 μm HEMT. Since the device model for the 0.25 μm HEMT with the mushroom gate profile was not available then, the amplifier was designed based on the 0.25 μm HEMT with the triangular gate profile. Fig. 4 shows the schematic layout of this amplifier, which uses shunt-shorted stubs and transmission lines as the input and output matching elements. The electrical lengths of the transmission lines are given at 40 GHz.

Both the input matching and the output matching network are bandpass-type filters with an order of 4. The input matching network has an upward frequency slope of

Manuscript received April 30, 1988; revised July 10, 1988.
The authors are with the Device Laboratory, Varian Research Center, Palo Alto, CA 94303.
IEEE Log Number 8823919.

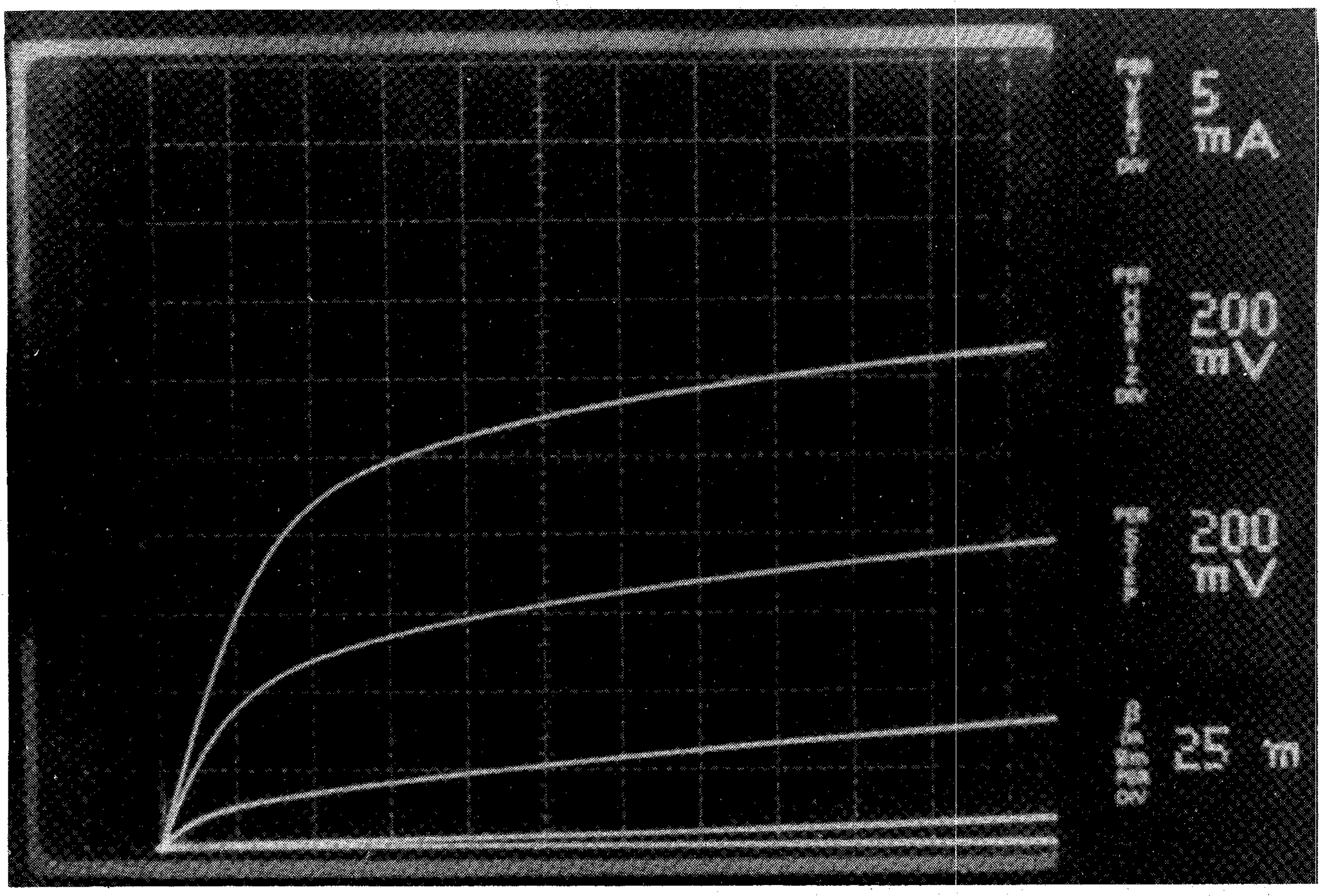

Fig. 2. *I–V* characteristics of 0.25 μm × 150 μm HEMT device.

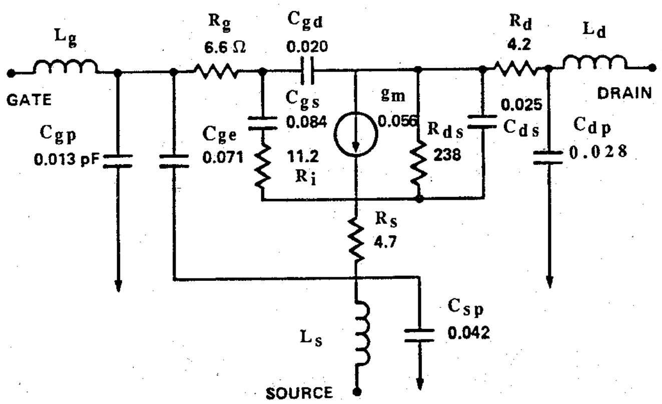

Fig. 3. Equivalent circuit model of 0.25 μm × 150 μm HEMT device biased for minimum noise condition.

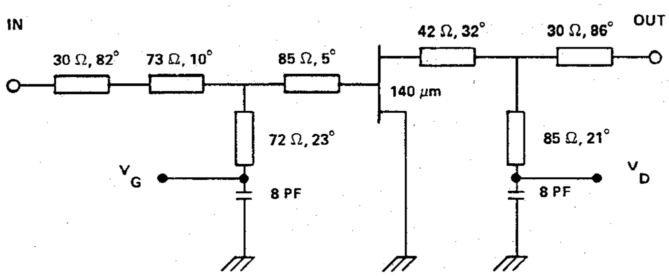

Fig. 4. Schematic circuit diagram for monolithic *Ka*-band amplifier. The electrical lengths of the transmission lines are given at 40 GHz.

4 dB/octave, a minimum insertion loss of 1 dB, and a 0.5 dB ripple from 20 to 40 GHz. The output matching network has an upward slope of 2 dB/octave and a minimum insertion loss of 1 dB with a 0.3 dB ripple. The gain slopes in the input and output matching networks compensate the 6 dB/octave gain roll-off of the HEMT device and result in a flat gain performance from 20 to 40 GHz. The minimized insertion losses in the input and output matching networks reduce the gain of the amplifier by 2 dB at 40 GHz.

Fifteen design parameters, including the matching and biasing circuit elements along with the gate periphery, were optimized for a maximum flat gain performance from 20 to 40 GHz using Supercompact. The discontinuities at the junctions of the matching elements were included in the simulation. The impedance of the matching elements was constrained to be within the range from 30 to 90 Ω for the purposes of practical realization and acceptable loss. A simulated gain of 6.5 dB from 20 to 42 GHz and input/output return losses of better than 5 dB from 30 to 50 GHz were obtained, as shown in Fig. 5. The minimum of the return loss occurs at 41 GHz, which is the upper limit of the desired bandwidth.

IV. Amplifier Fabrication

Standard processing techniques were used for most of the *Ka*-band HEMT amplifier fabrication. Isolation was

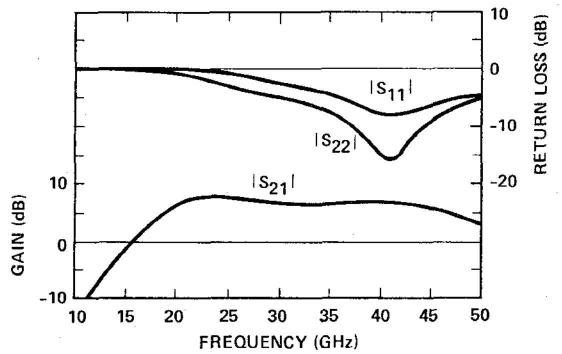

Fig. 5. Simulated gain and input/output return loss performances of the monolithic *Ka*-band amplifier.

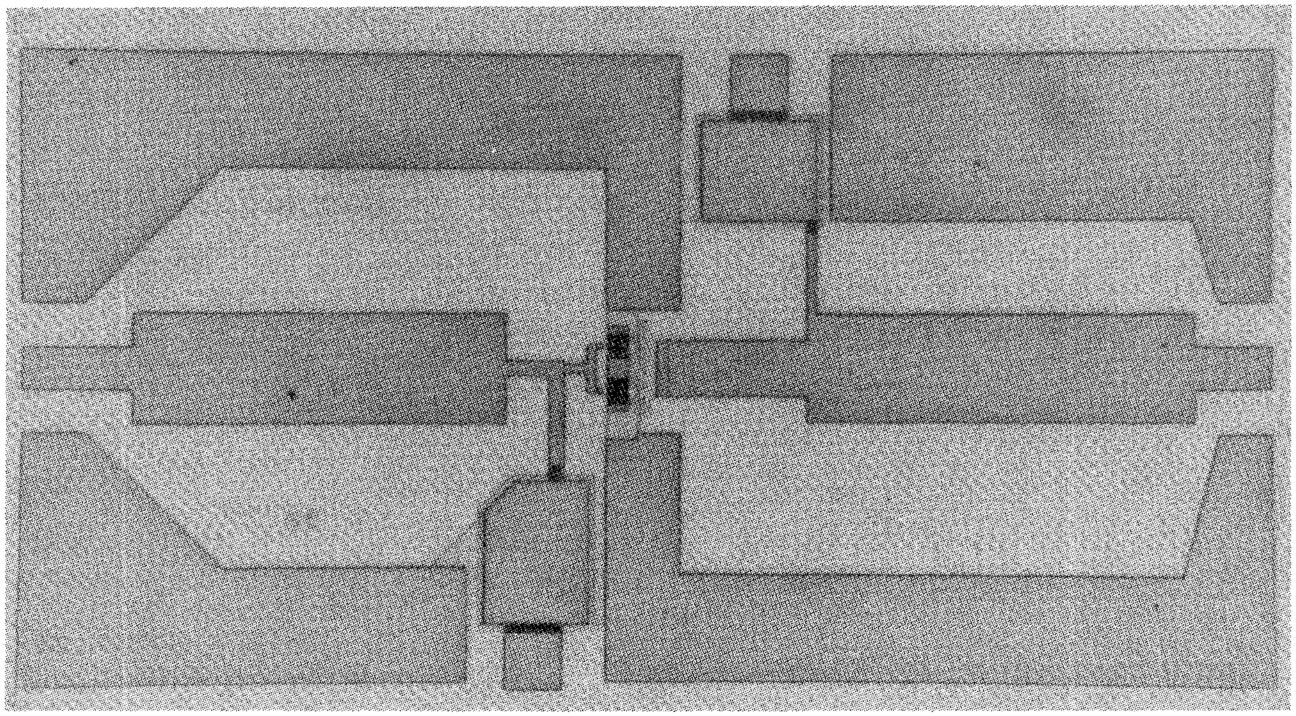

Fig. 6. Photograph of monolithic *Ka*-band amplifier. Chip size: 2.2 mm × 1.1 mm.

achieved with a 2500 Å mesa etch. The 0.25 μm gate was written with a Cambridge EBMF 10.5 E-beam machine using PMMA resist. The gate recess etch was a self-aligned wet etch process. The gate cross section was triangular, with a gate resistance of 470 Ω/mm. A sputtered SiO_2 layer of 2000 Å was used as the capacitor dielectric material. In order to achieve good RF grounding, 60 μm × 60 μm backside vias were incorporated using reactive ion etching. All other process steps used conventional metallization, lift-off, and pulse-plating techniques.

Fig. 6 shows a photograph of the *Ka*-band amplifier. The chip size is 2.2 mm × 1.1 mm, and the layout of the circuit is compatible with Cascade Microtech RF wafer probing.

V. Measured Gain Performance

A gain of approximately 6 dB from 20 to 38 GHz and an input return loss of better than 5 dB from 20 to 40 GHz (biased at V_{ds} = 3 V, V_{gs} = −0.3 V, and I_{ds} = 15 mA) were measured using the Cascade Microtech RF wafer prober, as shown by the solid curves in Fig. 7. Measurement was accomplished using the coax-based (2.4 mm) HP-8510B network analyzer with full error corrections from 10 to 40 GHz. The measured gain agrees well with the simulated result (Fig. 5), except at the high end of the band, where the measured gain starts to fall at 38 GHz. The shift in the frequency location of the minimum input return loss from 41 GHz (simulation) to 35 GHz (measurement) correlates with the earlier measured gain fall-off.

The HEMT device is particularly suited for achieving high gain because of its higher transconductance and lower output conductance (per unit g_m) compared with the MESFET. The higher transconductance is a result of the increased saturated velocity of the two-dimensional electron gas layer and the fact that AlGaAs can be doped

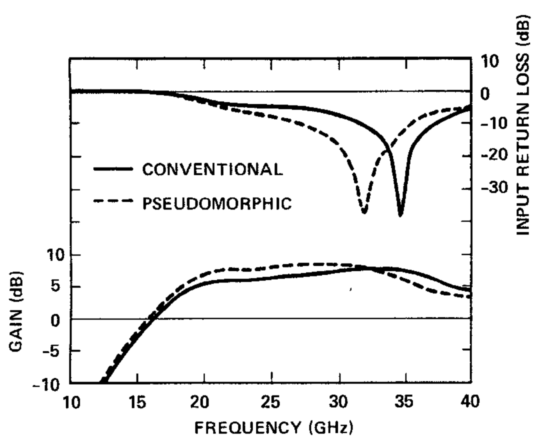

Fig. 7. Measured gain and input return loss performance of the monolithic *Ka*-band amplifier fabricated on conventional and pseudomorphic HEMT materials.

TABLE I
COMPARISON OF 0.25 μm MESFET, 0.25 μm HEMT, AND 0.25 μm PSEUDOMORPHIC HEMT CHARACTERISTICS

Device Type	MESFET	HEMT	Pseudomorphic HEMT
$g_m r_{ds}$	10	15	18
$f_t = g_m/(2\pi C_{gs})$ (GHz)*	44	56	58
f_{max} (GHz)+	70	101	104

*calculated values from device model.
+extrapolated from measured *MAG* value.

higher than GaAs without compromising the gate breakdown voltage (due to the larger bandgap). The lower output conductance is a result of the two-dimensional nature of the conduction electrons and the thinner epitaxial layer thickness, assuming the output resistance of a HEMT can be expressed in a way similar to that of a MESFET as [13]

$$r_{ds} \propto \cosh\left[\frac{\pi}{2}\left(\frac{L_g}{a}\right)\right]$$

where L_g is the gate length and a is the epitaxial layer thickness.

Ignoring feedback, the *MAG* of a FET is given by

$$MAG = \frac{g_m^2}{4\omega^2 C_{gs}^2 r_i g_{ds}} \propto \left(\frac{g_m}{C_{gs}}\right)^2 (g_m r_{ds})$$

assuming $r_i \propto g_m^{-1}$.

The 0.25 μm HEMT fabricated in our laboratory has a voltage gain factor $g_m r_{ds}$ of 15, compared to 10 for the 0.25 μm MESFET when biased for maximum gain, as listed in Table I. Furthermore, the cutoff frequencies f_t ($= g_m/2\pi C_{gs}$) for the 0.25 μm HEMT and MESFET are calculated to be 56 and 44 GHz, respectively, as listed in Table I. With a factor of 1.27 improvement in (g_m/C_{gs}) along with a factor of 1.5 improvement in $(g_m r_{ds})$, an approximate 3.8 dB gain improvement would be anticipated for the 0.25 μm HEMT compared to the 0.25 μm MESFET. The 0.3 μm $\times$ 150 μm gate length HEMT fabricated in our lab has an approximate 3 dB improvement in the measured associated gain performance over the MESFET of the same gate length [4], as shown in Fig. 8.

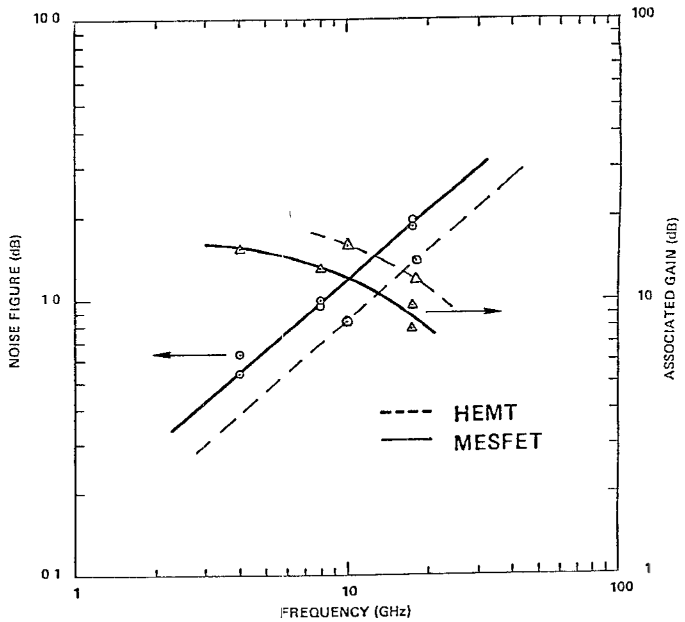

Fig. 8. Noise and associated gain performance comparison of 0.3 μm $\times$ 150 μm HEMT and MESFET.

VI. MEASURED NOISE FIGURE PERFORMANCE

The solid curve in Fig. 9 shows approximately 5 dB measured noise figure for the *Ka*-band amplifier from 26.5 to 40 GHz when biased at minimum noise bias condition. As stated previously, the amplifier was designed for flat gain rather than minimum noise figure performance. The amplifier noise figure was measured with a HP-R347B noise source and a HP noise measurement system using the waveguide test setup and the Cascade prober.

The HEMT device is known for its low-noise performance and its suitability for broad-band low-noise applications [4], [14]. The FET device can be characterized by a minimum intrinsic noise figure [14]:

$$F_{\min} = 1 + 2\frac{f}{f_c}\sqrt{PR(1 - C^2)}$$

where $f_c = (1/2\pi)(g_m/C_{gs})$ is the cutoff frequency, P and R are two dimensionless parameters which depend on biasing conditions and device parameters, and C is the correlation coefficient between the gate and drain noise sources.

The lower noise figure performance for HEMT's compared to MESFET's (as shown in Fig. 8) is due to the higher cutoff frequency (i.e., higher g_m/C_{gs}), as described before, and the higher correlation coefficient between the drain and gate noise current sources, subtracting partially the gate noise from the drain noise and reducing the intrinsic noise figure in the HEMT [14].

In addition, the noise figure for a FET device can be

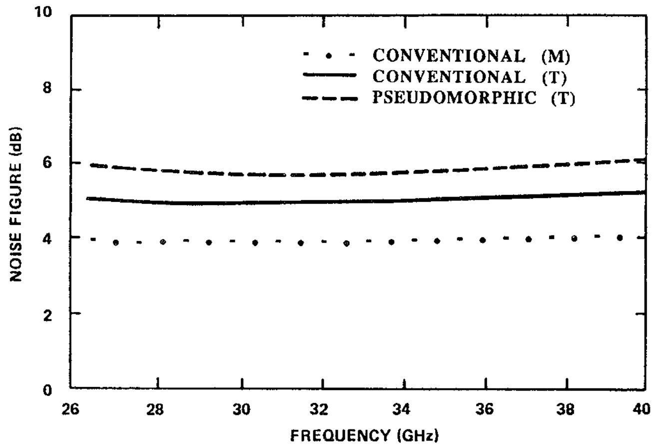

Fig. 9. Measured noise figure performance of the monolithic *Ka*-band amplifier fabricated on conventional and pseudomorphic HEMT materials. M and T represent mushroom and triangular gate profiles, respectively.

expressed by

$$F = F_{\min} + \frac{g_n}{R_0} \left| Z_0 - Z_{\text{opt}} \right|^2$$

where $F_{\min}$ is the minimum noise figure, g_n is the noise conductance, $Z_0 = R_0 + jX_0$ is the source impedance, and Z_{opt} is the optimized source impedance for minimum noise. The HEMT's have a lower noise conductance, which results in reduced sensitivity of the noise figure to changes in source impedance and therefore permits low-noise performance over a wider bandwidth [4], [14].

VII. Performance of Amplifier with Mushroom Gate Profile

A 0.25 μm gate with a mushroom gate profile has been developed recently using the trilevel resist and E-beam lithography. Fig. 10 shows a SEM photograph of a typical mushroom gate profile. The gate resistance of a 0.25 μm gate with a mushroom gate profile (70 Ω/mm) is reduced to almost 1/7 that for a 0.25 μm gate with a triangular gate profile (470 Ω/mm).

The 0.25 μm $\times$ 150 μm Π-configured HEMT with a mushroom gate profile has a measured noise figure of 1 $\pm$ 0.25 dB and an associated gain of 13 dB at 18 GHz. These data are comparable to those reported by others [11] for a 0.25 μm $\times$ 150 μm T-configured HEMT, which has a measured noise figure of 0.7 dB and an associated gain of 13.8 dB at 18 GHz.

A *Ka*-band amplifier with a mushroom gate profile was fabricated on conventional HEMT material. This amplifier gave 8 dB of gain from 20 to 37 GHz and a 4 dB noise figure (shown in Fig. 9 as dot–dash curve) over the whole *Ka*-band. These are the best reported results for a MMIC amplifier over this bandwidth. Compared to the amplifier with a triangular gate profile, the amplifier with the mushroom gate profile has 2 dB higher gain and 1 dB lower noise figure in the *Ka*-band, due to the higher g_m and lower R_g of the device.

VIII. Pseudomorphic HEMT Amplifier Performance

Excellent dc and millimeter-wave performance for the InGaAs/AlGaAs pseudomorphic HEMT's has recently been reported [15]–[17]. The advantages of the pseudomorphic HEMT include the elimination of deep trap effects through the use of low Al mole fraction, reduction in trap-related generation–recombination noise, high sheet charge density, higher mobility and velocity, and improved carrier confinement. Therefore, submicron gate pseudomorphic HEMT's are expected to have superior potential as low-noise and high-power devices in the millimeter-wave region.

A 0.25 μm $\times$ 150 μm pseudomorphic HEMT with a triangular gate profile was processed on the InGaAs/AlGaAs pseudomorphic HEMT material with 22 percent Al mole fraction and 18 percent In mole fraction grown by MBE in our laboratory, as shown in Fig. 11. These devices have a measured noise figure of 1.4 dB and an associated gain of 12.5 dB at 18 GHz, values comparable to those measured for a conventional HEMT. The 0.25 μm pseudomorphic HEMT has a voltage gain factor $g_m r_{ds}$ of approximately 18, a calculated cutoff frequency f_t of 58 GHz, and an extrapolated $f_{\max}$ of 104 GHz, as listed in Table I.

The *Ka*-band amplifier with a triangular gate profile was processed on the InGaAs/AlGaAs pseudomorphic HEMT material. A gain of 7.5 dB from 20 to 35 GHz and an input return loss of better than 5 dB from 20 to 40 GHz were measured, as shown by the dashed curves in Fig. 7. The 1.5 dB gain improvement for the pseudomorphic HEMT amplifier relative to the conventional HEMT amplifier is attributed mainly to the higher g_m (due to higher electron velocity) and lower g_{ds} (due to better carrier confinement) of the device. The earlier gain falloff for the pseudomorphic HEMT amplifier is related to the higher C_{gs} of the device.

The measured noise figure for the pseudomorphic HEMT amplifier is about 6.0 dB from 26.5 to 40 GHz, as shown by the dashed curve in Fig. 9, which for some reason is 1 dB higher than that for the conventional HEMT amplifier.

IX. Measured Output Power Performance

The 1 dB compression power was measured for the HEMT and pseudomorphic HEMT amplifiers at 30 GHz. When biased at maximum power, the 1 dB compression power for the HEMT amplifier was measured to be 10 dBm at 30 GHz. For close to the same bias current and voltage, the pseudomorphic HEMT amplifier has a 1 dB compression power around 11.5 dBm when biased for maximum power. Presumably, the higher value for the pseudomorphic HEMT version is due to the lower and sharper knee voltage.

X. Discussion and Conclusions

A monolithic low-noise amplifier using HEMT technology for the active device has been developed for *Ka*-

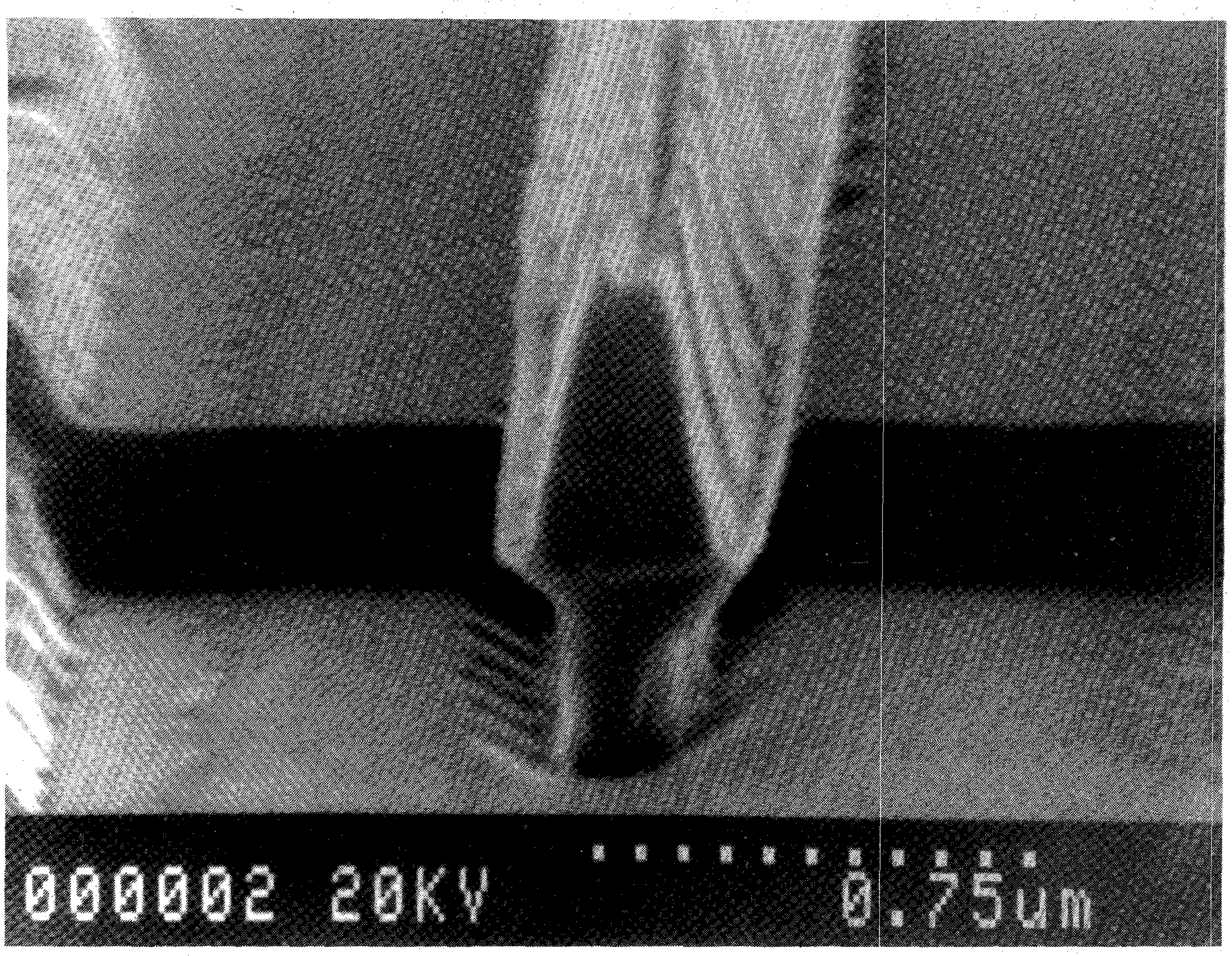

Fig. 10. SEM photograph of a typical mushroom gate profile.

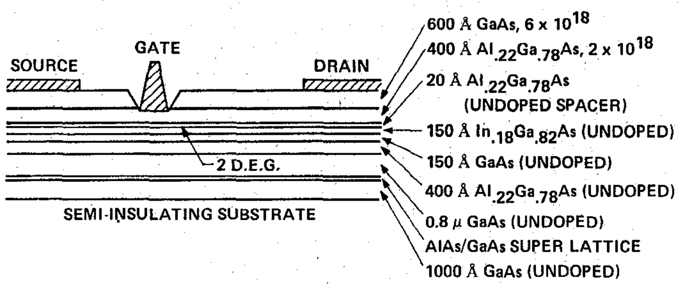

Fig. 11. Cross section of pseudomorphic HEMT structure.

band with about 6 dB gain from 20 to 38 GHz and approximately 5 dB for the noise figure from 26.5 to 40 GHz. By replacing the triangular gate profile with a mushroom gate profile, the amplifier achieved 8 dB gain from 20 to 37 GHz, with a 4 dB noise figure from 26 to 40 GHz. These are the best reported results for a MMIC amplifier over this bandwidth.

The same amplifier with a triangular gate profile was fabricated on pseudomorphic HEMT material and achieved 7.5 dB gain from 20 to 35 GHz with a 6.0 dB noise figure from 26.5 to 40 GHz.

The pseudomorphic HEMT amplifier has a 1 dB compression power of 11.5 dBm at 30 GHz, which is 1.5 dB higher than that for the conventional HEMT amplifier.

Devices with shorter gate length (i.e., 0.1 μm) have been developed using E-beam lithography, which will improve the gain and noise performance of the amplifier further.

Using the current 0.25 μm HEMT with a mushroom gate profile along with the improved circuit topology designed for minimum noise, a noise figure below 3 dB from 20 to 40 GHz for a broad-band MMIC amplifier should be achievable. With further improvement in the noise figure of the device (for example, a 0.1 μm HEMT with a mushroom gate profile), the noise figure of the *Ka*-band MMIC amplifier can be reduced even further.

Acknowledgment

The authors would like to acknowledge the technical support given by B. Knapp and C. Shih. They also wish to thank Z. Tan for his assistance in the E-beam lithography.

References

[1] J. J. Berenz, W. Nakamo, and K. Weller, "Low noise high electron mobility transistors," in *IEEE 1984 Microwave and Millimeter-Wave Monolithic Circuits Symp. Dig.*, p. 83.

[2] P. M. Smith *et al.*, "Advances in HEMT technology and applications," in *1987 IEEE MTT-S Int. Microwave Symp. Dig.*, p. 749.

[3] A. K. Gupta *et al.*, "Low noise high electron mobility transistors for monolithic microwave integrated circuits," *IEEE Electron Device Lett.*, vol. EDL-6, pp. 81–82, Feb. 1985.

[4] S. Bandy *et al.*, "A 2–20 GHz high-gain monolithic HEMT distributed amplifier," *IEEE Trans. Microwave Theory Tech.*, vol. MTT-35, p. 1494, Dec. 1987.

[5] Y. Ito, "0.8 to 18.0 GHz hybrid distributed amplifier using 0.25 × 200-μm MESFET and HEMT," in *Proc. 1987 Int. European Microwave Symp.*, p. 832.

[6] R. G. Pauley, P. G. Asher, J. M. Schellenberg, and H. Yamasaki, "A 2 to 40 GHz monolithic distributed amplifier," in *GaAs IC Symp. 1985 Tech. Dig.*, p. 15.

[7] M. J. Schindler, J. P. Wendler, A. M. Morris, and P. A. Lamarre, "A 15 to 45 GHz distributed amplifier using 3 FETs of varying periphery," in *GaAs IC Symp. 1986 Tech. Dig.*, p. 67.

[8] L. C. T. Liu, P. Riemenschneider, S. K. Wang, and H. Kanber, "A 30 GHz monolithic two stage low noise amplifier," in *GaAs IC Symp. 1985 Tech. Dig.*, p. 7.

[9] S. Bandla *et al.*, "A 35 GHz monolithic MESFET LNA," in *Proc. IEEE MTT 1988 Microwave and Millimeter-Wave Monolithic Circuits Symp.*, p. 151.

[10] K. Shibata, B. Abe, S. Hori, and K. Kamei, "Broadband HEMT amplifier for 26.5–40.0 GHz," in *1987 IEEE MTT-S Dig.*, p. 1011.

[11] K. H. G. Duh *et al.*, "Millimeter-wave low-noise HEMT amplifiers," in *1988 IEEE MTT-S Int. Microwave Symp. Dig.*, p. 923.

[12] J. M. Schellenberg, M. V. Maher, S. K. Wang, K. G. Wang, and K. K. Yu, "35 GHz low noise HEMT amplifier," in *1987 IEEE MTT-S Dig.*, p. 44.

[13] R. A. Pucel, H. A. Haus, and H. Statz, "Signal and noise properties of gallium arsenide microwave field effect transistors," in *Advances in Electronics and Electron Physics*, vol. 38, L. Marton, Ed. New York: Academic, 1975, p. 195.

[14] A. Cappy, "Noise modeling and measurement techniques," *IEEE Trans. Microwave Theory Tech.*, vol. 36, pp. 1–10, Jan. 1988.

[15] T. Henderson *et al.*, "Microwave performance of a quarter-micrometer gate low noise pseudomorphic InGaAs/AlGaAs modulation-doped field effect transistor," *IEEE Electron Device Lett.*, vol. EDL-7, p. 649, Dec. 1986.

[16] A. W. Swanson, "Millimeter-wave transistors—The pseudomorphic HEMT," *Microwaves and RF*, p. 139, Mar. 1987.

[17] P. C. Chao *et al.*, "0.1-μm gate-length pseudomorphic HEMT's," *IEEE Electron Device Lett.*, vol. EDL-8, p. 489, Oct. 1987.

*

Cindy Yuen received the B.S. degree in physics in 1972 from Tsing Hua University in Taiwan and the M.S. and Ph.D. degrees in physics from Stanford University in 1974 and 1978, respectively.

From 1978 to 1982 she worked in the Radiation Division of Varian Associates, Inc., where she was involved in the designs of the electron linear accelerator and the microwave hyperthermia system. In 1982 she joined the Varian Associates Central Research Laboratories, where she is currently engaged in the development of GaAs monolithic microwave integrated circuits.

*

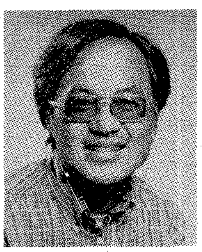

Clifford K. Nishimoto received the B.S. degree in electronic engineering from California Polytechnic State University at San Luis Obispo in 1973.

Currently, he is a process engineer at Varian Associates Research Center, Palo Alto, CA. He has been involved with the fabrication and testing of GaAs MESFET's, AlGaA/GaAs MODFET's, and HEMT MMIC's for microwave applications. His work has also included electron-beam lithography.

Michael Glenn (M'84) received the B.S.E.E. degree in 1980 from the University of Washington, Seattle, and the M.S.E.E. degree in 1986 from the University of Santa Clara, Santa Clara, CA.

Employed by the Wiltron Company from 1980 to 1985 as a Development Engineer for their Microwave Network Analyzer Group, he was involved in circuit design for microwave test instrumentation. Working for Avantek from 1985 to 1987, he developed computer-aided test systems primarily for the measurement of power and gain compression of microwave power devices and modules. Currently he is working at the Varian Research Center's MMIC Group, Palo Alto, CA, where he is involved in computer-aided measurement and characterization of microwave and millimeter-wave devices and circuits.

*

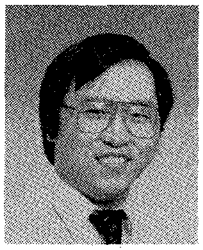

Yi-Ching Pao received the B.S. degree in electrophysics from National Chiao-Tung University in 1981 and the M.S.E.E. degree in 1983 from Pennsylvania State University.

In 1983, he joined Varian Associates, III–V Device Center, Santa Clara, CA, where he is currently in charge of the MBE operation and low-noise HEMT program. His research has involved developing GaAs/AlGaAs process and material growth of III–V semiconductor devices by MBE and high-electron-mobility transistors.

Mr. Pao is currently working toward the Ph.D. degree at Stanford University under the Honors Co-op program. He is a member of IEEE and Sigma Xi.

*

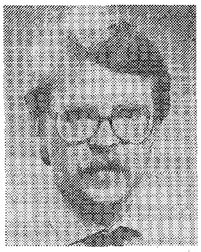

Ross A. LaRue received the B.S. degree in physics/mathematics at San Jose State University in 1977 and the M.S. degree in physics from the University of Illinois in 1979. He is currently an honors co-op student at Stanford University in the Applied Physics Department.

He joined Varian Associates in 1979 and worked for three years on novel high-efficiency III–V photovoltaic devices. In 1983, he began work in the microwave field and published an article on a distributed FET model. He is currently working on an HEMT version of the cascode distributed amplifier.

*

Robert Norton (M'87) received the Ph.D. degree in applied physics from Stanford University in 1983 with a dissertation on surface currents and hysteretic power dissipation in superconductors.

From 1979 to 1981, he was also with the magnetic bubble memory group at National Semiconductor Corporation, where he assisted in the design and development of 1- and 4-Mbit memory devices. Since 1983, he has been in the Microwave Group at the Varian Research Center, working on heterojunction device and process development, primarily with e-beam lithography.

Mary Day received the A.B. degree in geology from Occidental College, Los Angeles, CA, in 1977.

Since then she has been involved in many aspects of the process development of III–V microwave integrated circuits. Her main expertise is in high-resolution lithography and in thin-film deposition and etching technologies.

*

Irene Zubeck received the B.S. and M.S. degrees in materials science engineering from Stanford University in 1967 and 1982, respectively.

From 1965 to 1968 she was employed by the Stanford Research Institute, where she ran an X-ray measurement facility. From 1968 to 1971 she was with Chromatix, Inc., where she produced crystals for tunable lasers. From 1971 to 1976 she was employed by Stanford University, where she grew compound semiconductor materials. In 1976 she joined Varian Associates, where she has grown GaAs and InP by vapor epitaxy for devices and has also been involved in the processing of MMIC's. Her current interests are the development of metallization techniques and electron-beam lithography.

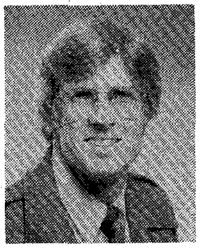

Steve G. Bandy received the B.S. degree in electrical engineering from Walla Walla College, College Place, WA, in 1965 and the Ph.D. degree in electrical engineering from Stanford University in 1970.

He joined the Varian Research Center of Varian Associates in Palo Alto, CA, in 1969 and has since been responsible for advanced studies on III–V discrete FET's for use in low-noise and power applications. In 1975, he was appointed Manager of the Microwave Device Group, and in 1985 he was appointed Manager of the Microwave Circuits and Devices Group of the Research Center.

Dr. Bandy is a member of Sigma Xi.

*

George A. Zdasiuk (S'80–A'80–M'81) received the B.Sc. degree in engineering science and the M.Sc. degree in physics from the University of Toronto in 1974 and 1975, respectively. He subsequently received the Ph.D. degree in applied physics from Stanford University in 1981. His thesis research was in the area of quantum electronics.

In 1980, he joined Varian Associates' Solid State Laboratory. He has been involved in the development of submicron GaAs FET devices, microwave characterization techniques, and the design and fabrication of GaAs monolithic microwave integrated circuits. Currently, he is the Associate Director of the Device Laboratory at Varian Research Center.

Dr. Zdasiuk is a member of the Institute of Electrical and Electronics Engineers and the American Physical Society.